Lasing in a three-dimensional photonic crystal of the liquid crystal blue phase II

WENYI CAO[1], ANTONIO MUÑOZ[2], PETER PALFFY-MUHORAY*[1] AND BAHMAN TAHERI[1]

[1]Liquid Crystal Institute, Kent State University, Kent, Ohio 44242, USA

[2]Dept. de Fisica, Universidad Autonoma Metropolitana, Mexico City 09340, Mexico

*e-mail: mpalffy@cpip.kent.edu

Published online: 9 September 2002; doi:10.1038/nmat727

Photonic-bandgap materials, with periodicity in one, two or three dimensions, offer control of spontaneous emission and photon localization[1–3]. Low-threshold lasing has been demonstrated in two-dimensional photonic-bandgap materials, both with distributed feedback and defect modes[4–9]. Liquid crystals with chiral constituents exhibit mesophases with modulated ground states. Helical cholesterics are one-dimensional, whereas blue phases are three-dimensional self-assembled photonic-bandgap structures[10]. Although mirrorless lasing was predicted[11,12] and observed in one-dimensional helical cholesteric materials[13,14] and chiral ferroelectric smectic materials[15], it is of great interest to probe light confinement in three dimensions. Here, we report the first observations of lasing in three-dimensional photonic crystals, in the cholesteric blue phase II. Our results show that distributed feedback is realized in three dimensions, resulting in almost diffraction-limited lasing with significantly lower thresholds than in one dimension. In addition to mirrorless lasing, these self-assembled soft photonic-bandgap materials may also be useful for waveguiding, switching and sensing applications.

The blue phases (BP) of cholesteric liquid crystals are thermodynamically stable, modulated phases in the temperature interval that occurs between the isotropic fluid and the helical cholesteric phases. Blue phase structures may be considered, to a good approximation, to consist of double-twist tubes, stacked in three dimensions with cubic symmetry[16,17] (Fig. 1), somewhat similar to the wood-pile[18] and scaffold[19] structures. The direction of average orientation of the molecular symmetry axis is axial in the centre of the tubes, but rotates with distance from the centre to develop an equal tangential component at the surface (Fig. 1a). Outside the double-twist tubes, the director cannot vary smoothly everywhere due to topological constraints, and disclination lines are formed (Fig. 1b). The unit cells are body-centred-cubic for BPI and simple cubic for BPII. Although the composition is spatially uniform, the anisotropic molecular polarizability and spatially varying orientation lead to periodic susceptibility modulations, and, if the lattice parameter is comparable to optical wavelengths, to strong Bragg reflections. The band-structure of BPs has not yet been completely determined. One calculation has been made[20] that models the dielectric structure for BPII by just two Fourier amplitudes in the basis set <100> and <110>. This approximate model predicts an incomplete bandgap for one circularly polarized mode.

We have carried out lasing experiments in BPII of the mixture consisting of the nematic liquid crystal E48 and the chiral dopant CB15 (both from EM Industries; used at 1:1.25 v/v%), and 1 wt% of the dye DCM (Aldrich) between untreated indium tin oxide (ITO)-coated glass plates separated by 23 μm mylar spacers. The samples showed the following phase sequence: helical cholesteric (23.2 °C), BPI (23.6 °C), BPII (24.4 °C) and isotropic fluid. These phases were identified using reflection polarizing microscopy. On slow cooling (0.001 °C min^{-1}.) from the isotropic phase, single crystals of BPII up to 150 μm in diameter were grown (Fig. 2 inset). We found that in our mixture, it was possible to grow larger single crystals of BPII on ITO-coated glass, which provides relatively weak anchoring, than on glass coated with buffed polyimide or on uncoated glass. The reflection spectrum shows peaks in the red, green and blue at 611 nm, 494 nm and 432 nm (Fig. 2, curve a). Using the Bragg relation and consistency considerations for reflected intensity, lattice parameters and direction of preferred crystal growth[17], we assign the (100) and (110) planes to the reflections at 611 nm and 432 nm, respectively. The origin of the broad reflection peak at 494 nm is not well understood, but has been attributed to internal oblique reflection[17]. At low temperatures in the helical state, the sample shows a single reflection band (Fig. 2, curve b). The reflected light is left-circularly polarized, with the

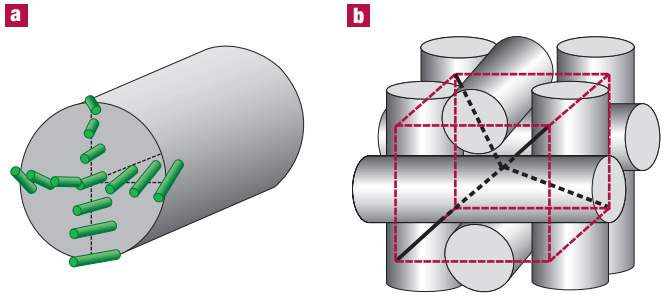

Figure 1 Schematic of the BPII structure. a, The director field inside a double-twist tube. **b**, Stacking of double-twist tubes and unit cell (red) and disclination lines (black). The unit cell is bounded by six planes that bisect the double-twist tubes. Disclination lines start at the centre of the unit cell, and continue to those four corners where the three nearest double-twist tubes in the unit cell form a coordinate system with the same handedness as the liquid crystal.

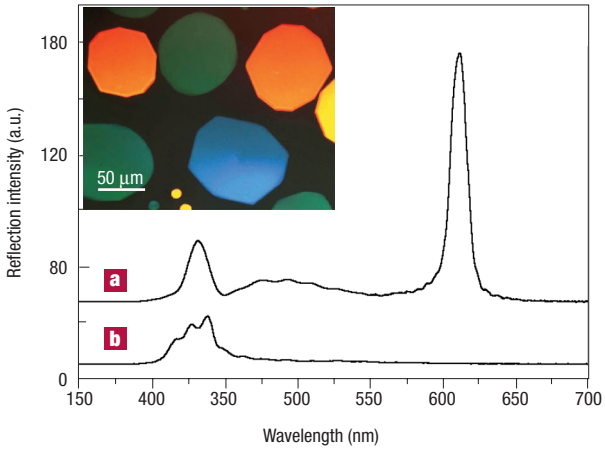

Figure 2 Reflection spectra of the liquid crystal/chiral dopant mixture E48:CB15 (1:1.25 v/v%). Curve **a**, BPII single crystals at 24.6 °C. Curve **b**, The helical state at 21.0 °C. The inset shows a micrograph of the BPII single crystals growing from the isotropic fluid phase (dark region). The micrograph was produced with a digital camera (MagnaFire-SP, Optonics) mounted on a polarizing microscope (Nikon Optiphot-Pol).

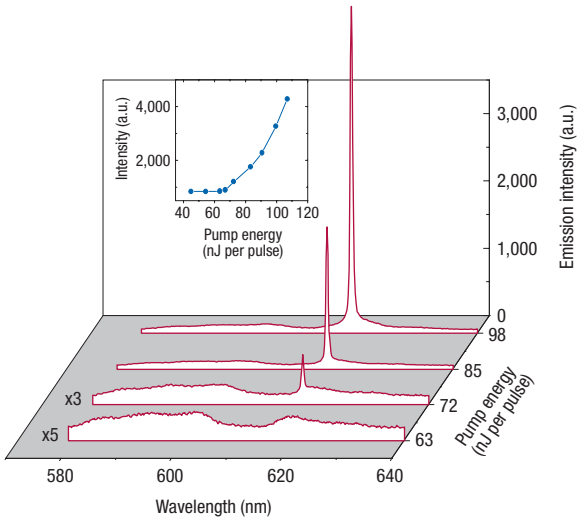

Figure 3 Fluorescence and lasing spectra at different pump energies. The inset shows the emitted intensity at a wavelength of 617.23 nm versus pump energy. The first two spectra are shown at x5 and x3 magnification for clarity.

same handedness as the chiral dopant CB15. The dissolved DCM dye has a broad fluorescence peak, centred at 610 nm, in both the isotropic and helical cholesteric states of the host.

The sample was pumped with 7.5 ns pulses at a wavelength of 532 nm from a Nd:YAG laser (Quantel YG682S-100). The pump beam, with a 23 µm waist, was focused on a region showing strong reflection at 611 nm, probably on a single BPII crystal with (100) orientation. The band structure of the BPII host modifies the fluorescence spectrum of the DCM dye; at low pump energies a dip in the emission occurs at the position of the (100) reflection peak (Fig. 3). A sharp lasing peak emerges at the low-energy band edge and grows to dominate the entire emission spectrum as the pump energy is increased. The lasing peak is at 617.23 nm, with a lorentzian lineshape and a full-width at half-maximum of 0.11 nm. A clear lasing threshold is seen at 78 nJ per pulse (Fig. 3 inset)—corresponding to a peak fluence of 19 mJ cm^{-2}—which is less than half the threshold for helical cholesteric samples with the same dye concentration and excitation conditions. Above the threshold, unstable lasing peaks can appear at the high-energy band edge or in the middle of the energy band. The laser emission is left-circularly polarized, which indicates optical feedback through internal Bragg reflection, and it is confined to a cone of ~0.12 rad (Fig. 4a inset). This is consistent with a diffraction-limited emission from a 13-µm-diameter disk.

The above results, for both pump and laser emission in the (100) direction, can be understood in terms of one-dimensional distributed feedback. However, we have also observed lasing in the (010) and (001) directions (Fig. 4a), which indicates distributed feedback in three dimensions. The configuration for excitation and detection is shown in Fig. 4b. To detect laser emission in the *y* and *z* directions, a single crystal domain at one corner of the cell is excited by the pump beam. This allows emission in the *y* and *z* directions to reach the detectors without reflection

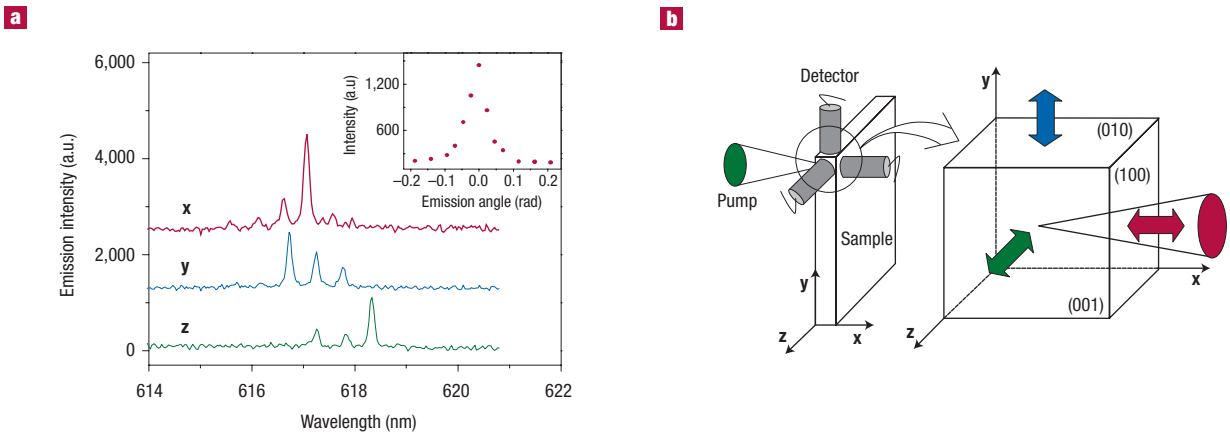

Figure 4 Lasing in three dimensions. a, Lasing spectra measured in the three orthogonal directions, *x*, *y* and *z*. The inset shows the spatial distribution of laser emission in the pump direction (*x* direction). **b**, The configuration used in measurements and schematics of (100), (010) and (001) planes of BPII and directions of laser emission (arrows).

or scattering by other domains. Furthermore, because the (010) and (001) planes of the BPII crystal do not necessarily coincide with the *y* and *z* directions, recrystallization of the BPII phase of sample has been carried out until the appropriate orientation of the domain is achieved, and detection of lasing is realized in three dimensions. The spectra show a major lasing peak in each of the *x*, *y* and *z* directions, occurring at slightly different wavelengths within 1.6 nm of each other. Because the lasing occurs at the edge of the reflection peak, the shifts of lasing wavelength suggest that periodicities in the *x*, *y* and *z* directions vary by approximately ± 0.13%. The emission spectra suggest coupling of orthogonal modes by Bragg diffraction[8] from the <110> planes, similar to recent observations of coupling of three non-parallel diffracted waves in a two-dimensional photonic crystal[6]. Strong coupling is consistent with the model[20] that uses a ratio of 0.6 for the Fourier amplitudes corresponding to the basis sets <110> and <100>. Our measured ratio of transverse to longitudinal major lasing intensities is 0.6.

The detected highly directional laser emissions in the *y* and z directions are not simply consequences of wave guiding in the sample. In one-dimensional helical cholesterics, lasing is observed only along the helix axis; in the orthogonal directions, the emission spectra are broad, as in the isotropic state.

We have demonstrated lasing, for the first time, in a three-dimensional photonic-bandgap material. Our results show that low-threshold three-dimensional lasing is possible even in materials with small and incomplete bandgaps. Self-assembling organic materials such as liquid crystals may therefore be useful for a variety of photonic-bandgap applications.

Received 8 July 2002; accepted 22 August 2002; published 9 September 2002.

References

1. Yablonovitch, E. Inhibited spontaneous emission in solid-state physics and electronics. *Phys. Rev. Lett.* **58,** 2059–2062 (1987).
2. John, S. Strong localization of photons in certain disordered dielectric superlattices. *Phys. Rev. Lett.* **58,** 2486–2489 (1987).
3. Busch, K. & John, S. Liquid crystal photonic-band-gap materials: the tunable electromagnetic vacuum. *Phys. Rev. Lett.* **83,** 967–970 (1999).
4. Painter, O. *et al.* Two-dimensional photonic band-gap defect mode laser. *Science* **284,** 1819–1821 (1999).
5. Mekis, A., Meier, M., Dodabalapur, A., Slusher, R. E. & Joannopoulos, J. D. Lasing mechanism in two-dimensional photonic crystal lasers. *Appl. Phys. A: Mater.* **69,** 111–114 (1999).
6. Notomi, M., Suzuki, H. & Tamamura, T. Directional lasing oscillation of two-dimensional organic photonic crystal lasers at several photonic bandgaps. *Appl. Phys. Lett.* **78,** 1325–1327 (2001).
7. Susa, N. Threshold gain and gain-enhancement due to distributed-feedback in two-dimensional photonic-crystal lasers. *J. Appl. Phys.* **89,** 815–823 (2001).
8. Riechel, S., Kallinger, C., Lemmer, U. & Feldmann, J. A nearly diffraction limited surface emitting conjugated polymer laser utilizing a two-dimensional photonic band structure. *Appl. Phys. Lett.* **77,** 2310–2312 (2000).
9. Rocha, L. *et al.* Laser emission in periodically modulated polymer films. *J. Appl. Phys.* **89,** 3067–3069 (2001).
10. Etchegoin, P. Blue phase cholesteric liquid crystals as thermotropic photonic crystals. *Phys. Rev. E* **62,** 1435–1437 (2000).
11. Goldberg, L. S. & Schnur, J. M. Tunable internal feedback liquid crystal laser. US patent 3,771,065 (1973).
12. Il'chshin, I. P., Tikhonov, E. A., Tishchenko, V. G. & Shpak, M. T. Generation of a tunable radiation by impurity cholesteric liquid crystals. *J. Exp. Theor. Phys. Lett.* **32,** 24–27 (1981).
13. Kopp, V. I., Fan, B., Vithana, H. K. M. & Genack, A. Z. Low-threshold lasing at the edge of a photonic stop band in cholesteric liquid crystals. *Opt. Lett.* **23,** 1707–1709 (1998).
14. Muñoz, A., Palffy-Muhoray, P. & Taheri, B. Ultraviolet lasing in cholesteric liquid crystals. *Opt. Lett.* **26,** 804–806 (2001).
15. Ozaki, M., Kasano, M., Ganzke, D., Haase, W. & Yashino, K. Mirrorless lasing in a dye-doped ferrolectric liquid crystal. *Adv. Mater.* **14,** 306–309 (2002).
16. Crooker, P. P. in *Chirality in Liquid Crystals* (eds Kitzerow, H. & Bahr, C.) 186–222 (Springer, New York, 2001).
17. Stegemeyer, H., Blumel, Th., Hiltrop, K., Onusseit, H. & Porsch, F. Thermodynamic, structural and morphological studies on liquid-crystalline blue phase. *Liq. Cryst.* **1,** 3–28 (1986).
18. Sözüer, H. S. & Dowling, J. P. Photonic band calculations for woodpile structures. *J. Mod. Optic.* **41,** 231–239 (1994).
19. Sözüer, H. S. & Haus, J. W. Photonic bands: simple-cubic lattice. *J. Opt. Soc. Am. B* **10,** 296–302 (1993).
20. Hornreich, R. M. & Shtrikman, S. Photonic bands in simple and body-centred-cubic cholesteric blue phase. *Phys. Rev. E* **47,** 2067–2072 (1993).

Acknowledgements

We acknowledge discussions with D.-K. Yang. This work was supported by the US National Science Foundation through DMR-0132611.
Correspondence and requests for materials should be addressed to P.P-M.

Competing financial interests

The authors declare that they have no competing financial interests.